Electronic supplementary information

Lysosome-targeting pH indicator based on peri-fused naphthalene monoimide with superior stability for long term live cell imaging

Astrid Tannert, [a,b] Javier Garcia Lopez, [d,f] Nikolay Petkov, [e] Anela Ivanova, [e] Kalina Peneva, [d,f] and Ute Neugebauer *[a,b,c,e,f]

[a.] *Leibniz Institute of Photonic Technology, Albert-Einstein-Str. 9, 07745 Jena, Germany*
[b.] *Center for Sepsis Control and Care, Jena University Hospital, Am Klinikum 1, 07747 Jena, Germany.*
[c.] *Institute of Physical Chemistry and Abbe School of Photonics, Friedrich Schiller University Jena, Helmholtzweg 4, 07743 Jena, Germany.*
[d.] *Institute of Organic Chemistry and Macromolecular Chemistry, Friedrich Schiller University Jena, Lessingstraße 8, 07743 Jena, Germany.*
[e.] *Faculty of Chemistry and Pharmacy, Sofia University "St. Kliment Ohridski", 1 James Bourchier blvd., Sofia, Bulgaria*
[f.] *Jena Center of Soft Matter (JCSM), Friedrich Schiller University Jena, Philosophenweg 7, 07743 Jena, Germany.*

* corresponding author, email: ute.neugebauer@leibniz-ipht.de

Synthetic procedures

General experimental details

Starting materials and solvents were purchased from Merck, Fluka, Fisher Scientific and Sigma Aldrich; they were used without further purification. All reactions were monitored by thin-layer chromatography, using Merck TLC Silica gel 60 F254 on aluminium sheets. Purifications by column chromatography were performed using Macherey-Nagel silica gel 60 (0.04 - 0.066 mm). Flash chromatography was performed using a puriFlash® XS520Plus purification system. Reactions under microwave irradiation were carried out in a Biotage® Initiator Classic microwave reactor. NMR analysis (^{1}H and 13C^{1}H) was carried out with a Bruker Avance 300 MHz spectrometer. High-resolution mass spectra (HRMS) were recorded with a Finnigan MAT95XL using a micro ESI device. Accurate masses were obtained using the peak matching algorithm and Ultramark 1622 as standard.

Compounds **1 - 4** (as depicted in Scheme 1, main manuscript, for the synthesis of the naphthalene monoamide fluorophore peri-fused with a guanidinium group) were prepared as described previously. [1, 2]

N,*N*,*N*-tributyl-6-(2-imino-6,8-dioxo-1,3,6,8-tetrahydropyrido[3,4,5-*g,h*]perimidin-7(2*H*)-yl) hexan-1-aminium bromide (**NMI-LS**): 7-(6-bromohexyl)-2-imino-2,3-dihydropyrido[3,4,5-*g,h*] perimidine-6,8(1*H*,7*H*)-dione (**4**, 150 mg, 0.361 mmol) was suspended in 1,2-dichlorobenzene (5 ml) in a microwave reactor tube equipped with a magnetic stirrer. Then, tributylamine (858 µL, 3.61 mmol, 10 equiv.) was added and the reaction mixture was sealed under argon and irradiated at 200W (160 ºC) for 3 hours. After cooling to room temperature the crude mixture was poured in diethyl ether (150 ml) and the brown-yellowish precipitate formed was filtered off and washed with diethyl ether (100 mL). The crude material was purified by flash chromatography (CH_2Cl_2/ methanol 10:1 to 7:3), yielding 34.7 mg (57.8 µmol, 17%) as a yellow solid.

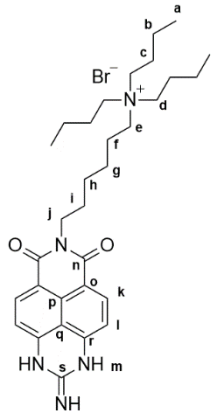

R_f=0.29 (CH_2Cl_2/ MeOH 7:3);

^{1}H-NMR (300 MHz, 25 °C, DMSO-d_6): δ = 8.10 (d, *J* = 9.0 Hz, 2H k), 7.84 (s, 2H m), 6.75 (d, *J* = 9.0 Hz, 2H l), 3.93 (t, *J* = 6.0 Hz, 2H e), 3.70 (q, *J* = 6.0 Hz, 2H j), 3.17 (t, *J* = 12.0 Hz, 6H d), 1.58- 1.53 (m, 10H c, f, i), 1.34- 1.25 (m, 10H b, g, h), 0.91 (t, *J* = 6.0 Hz, 9H a).

^{13}C-NMR (75 MHz, 25 °C, DMSO-d_6): δ = 163.26 (n), 154.28 (s), 134.49 (r), 130.52 (k), 114.00 (p), 109.86 (o), 62.81 (q), 60.83 (d), 49.02 (l), 47.96 (e), 30.89 (j), 30.80 (f), 28.00 (i), 26.84 (h), 25.66 (g), 23.82 (c), 19.66 (b), 13.93 (a).

HRMS (ESI+): *m/z* expected for $[C_{31}H_{46}N_5O_2]^+$ = 520.36515; observed 520.36303.

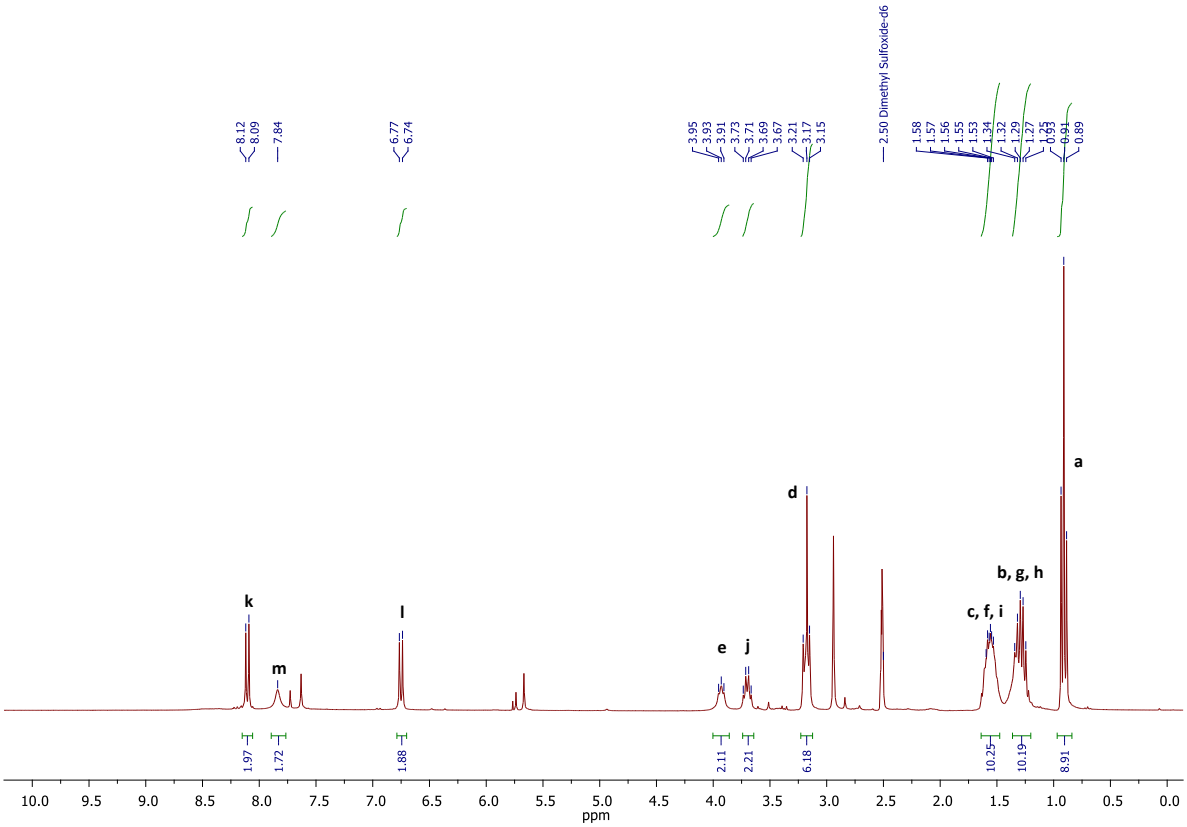

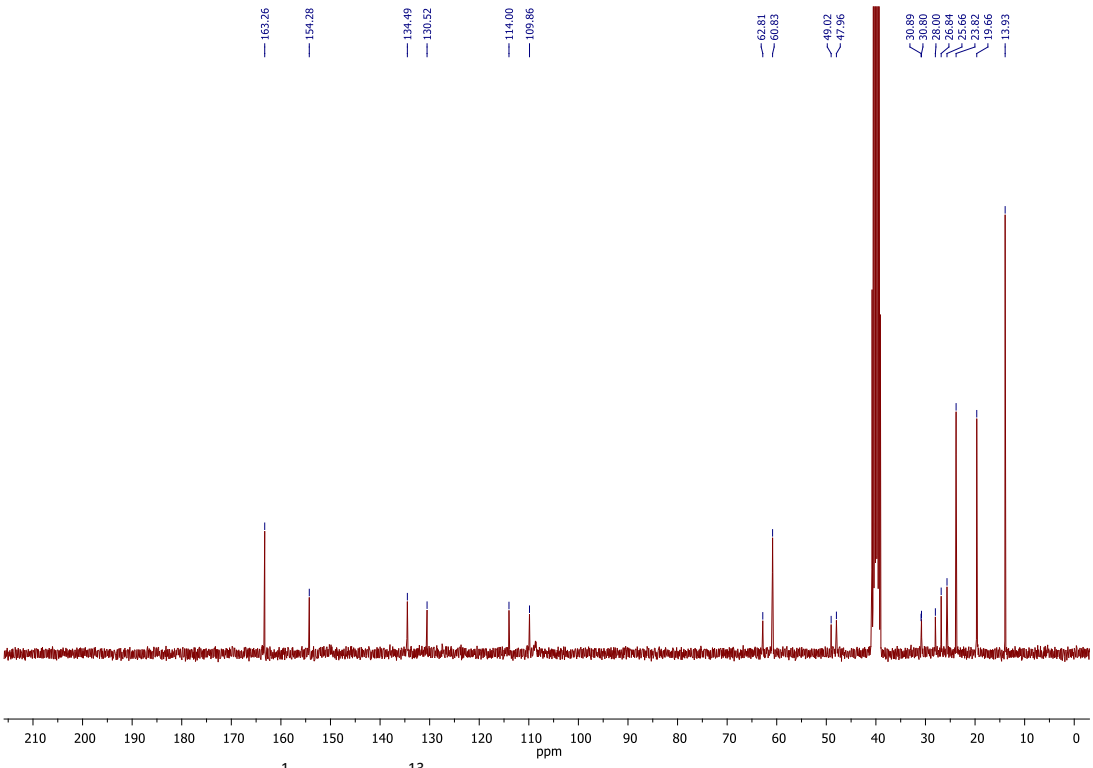

^{1}H-NMR and ^{13}C-NMR spectra of compound **NMI-LS** in DMSO-d_6.

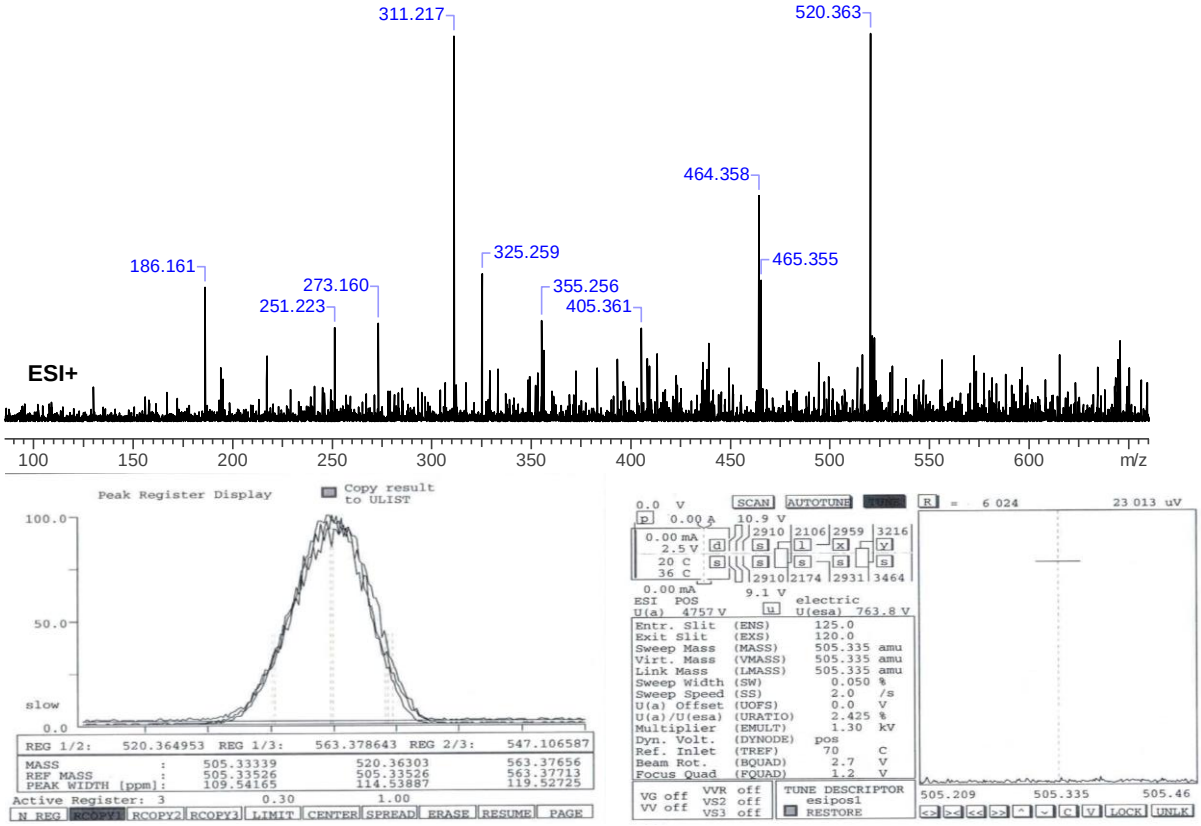

NMI-LS was measured dissolved in methanol, ion mode: ESI+. Fragmentation found: 520 $[M\text{-}Br]^+$, 464 $[M\text{-}Br\text{-}But]^+$,405 $[M\text{-}Br\text{-}2But]^+$, 311 $[M\text{-}Br\text{-}Gua\text{-}Naph\text{-}CO]^+$, 251 $[M\text{-}Br\text{-}(CH_2)_6NBut_3]^+$ McLafferty rearrangement, 186 $[NBut_3]^+$.

Table S1: Literature overview on lysosomal-targeted pH-sensitive dyes

structure	spectral range	readout	range of pH sensitivity	labelling time (concentration)	long term stability in cells	investigated biological samples	notes	references
NMI-LS 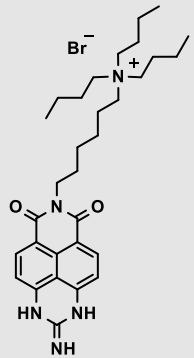	λ_{ex}=400-490 nm λ_{em}= 450-530 nm	excitation ratio 458 nm /405 nm OR emission ratio 467 nm /449 nm OR average fluorescence lifetime	2-6	30 min (0.5 µM)	48 h	HeLa cells	two photon excitation and FLIM readout possible	this publication
FITC-labeled dextran 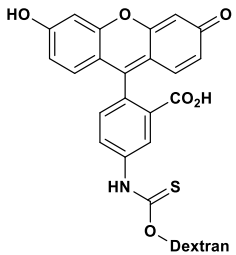	λ_{ex}=450-495 nm λ_{em}= 510-530 nm	excitation ratio 495 nm /450 nm OR emission ratio 515 nm /610 nm	4-7	16 h -3 d (1 mg /ml)	several days	mouse macrophages, human fibroblasts	commercially available	[3-5]
glyco- fluorescein/rhodamine-X-lactam probes	λ_{ex}=495 nm (fluorescein) λ_{ex}=595 nm (rhodamine-X-lactam) λ_{em}= 535 nm (fluorescein) λ_{em}=620 nm (rhodamine-X-lactam)	emission ratio (with changing excitation) 515 nm /610 nm (pH range 4-5) and 610 nm / 515 nm (pH range 5-7.5)	4-7.5	24 h (20 µM)	after 24 h superior retention compared to LysoTracker™ Red, also retention when acidity is lost	HeLa, U2OS and other cell lines	dual wavelength excitation needed, no simultaneous acquisition of both emission peaks possible, i.e. artifacts by fast moving organelles might be induced in microscopy	[6]

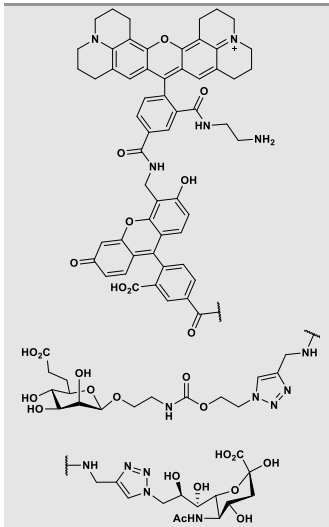								
benzimidazole-based probe 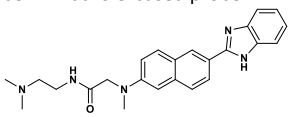	λ_{ex}=360 nm λ_{ex}=740 nm (two photon exc.) λ_{em}= 400-550nm; λ_{em}= 500-550nm (green channel) λ_{em}=474 nm (isoemission point)	emission ratio I_{green} / I_{iso}	5-7	30 min (3 µM)	not determined	HeLa cells, hippocampal slices	two-photon excitation possible	[7]
carbazole-based probes 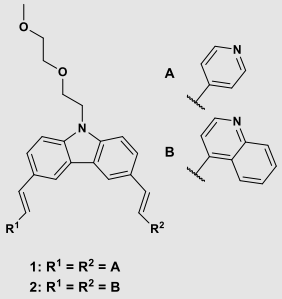	λ_{ex}=390-490 nm λ_{ex}=760 nm (two photon exc.) λ_{em}= 450-525nm (ch1, probe A) λ_{em}= 575-650nm (ch2, probe A) λ_{em}= 500-550nm (ch1, probe B) λ_{em}= 625-700nm (ch2, probe B)	emission ratio I_{ch2} / I_{ch1}	4-5 (probe A) 4.5-5.5 (probe B)	30 min (30 µM)	not determined	HeLa cells	two-photon excitation possible	[8]
naphthalene-naphthalimide-based probe	λ_{ex}=405nm λ_{ex}=760 nm (two photon exc.)	emission ratio I_{ch2} / I_{ch1}	3-6.5	60 min (1 µM)	not determined	HeLa cells, living tissue, zebrafish	FRET-based, two-photon excitation possible	[9]

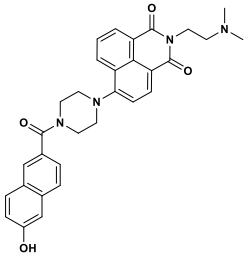	λ_{em}= 415-475nm (ch1) λ_{em}= 495-540nm (ch2)							
naphthalimide-rhodamine-based probe 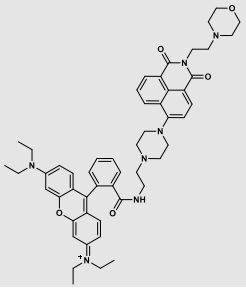	λ_{ex}=390-500nm λ_{ex}=780 nm (two photon exc.) λ_{em}= 400-550nm (ch1, deprotonated form) λ_{em}= 550-700nm (ch2, protonated form)	emission ratio I_{ch2} / I_{ch1} or I_{ch1} / I_{ch2}	4-6	30 min – 6 h (1-10 µM)	not determined	HeLa cells, zebrafish	FRET-based, two-photon excitation possible	[10] [11]
quinolone-based probe 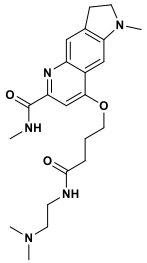	λ_{ex}=405 nm λ_{em}= 430-510nm (green, de-protonated form) λ_{em}= 520-600nm (yellow, protonated form)	emission ratio I_{green} / I_{yellow} (appr. 494 nm / 570 nm)	4-6	30 min (2 µM)	not determined	NIH 3T3 cells		[12]
naphthalimide-coumarin-based probe 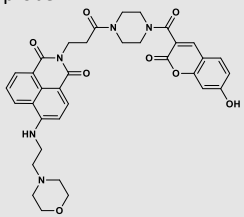	λ_{ex}=380- 405 nm, λ_{ex}=380- 500 nm (protonated form) λ_{em}= 420-650nm	emission ratio 530 nm /454 nm (pH range 4-6) and 454 nm / 530 nm (pH range 6-8)	4.5-8	10 min (5 µM)	not determined	HeLa cells	FRET-based	[13]
chromenoquinoline-based probe	λ_{ex}=350- 470 nm,	emission ratio I_{red} / I_{green}	4-6.5	15 min (5 µM)	not determined	HeLa cells		[14]

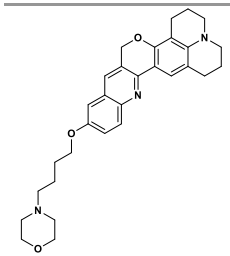	λ_{ex}=350- 580 nm, (protonated form) λ_{em}= 515-550nm (green, de-protonated form) λ_{em}= 570-620nm (red, protonated form)	(appr. 613 nm /560 nm)						
porphyrin-pyranine-based probe 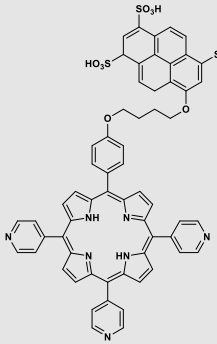	λ_{ex}=405 nm λ_{em}= 400-500nm (blue) λ_{em}= 620-750nm (red)	emission ratio I_{red} / I_{blue} (appr. 660 nm / 435 nm)	2.5-8.5	30 min (7.5 µM)	not determined	A549 cells		[15]
coumarin-rhodamine-based probe 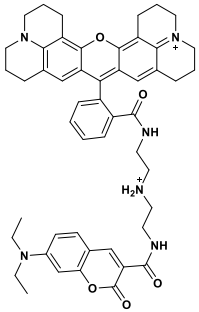	λ_{ex}=405 nm (coumarin), λ_{ex}=561 nm (rhodamine) λ_{em}= 410-490nm (green, coumarin) λ_{em}= 593-735nm (red, rhodamine)	emission ratio I_{red} / I_{green} (appr. 605 nm /475 nm)	4.5-7	30 min (3 µM)	not determined	HeLa cells	coumarin is always on, rhodamine activatable by acidity; dual wavelength excitation needed, no simultaneous acquisition of both emission peaks possible, i.e. artifacts by fast moving organelles might be induced in microscopy	[16]
BODIPY-based probes	λ_{ex}=500-650 nm (probe A) λ_{ex}=550-750 nm (probe B) λ_{em}= 515-565nm (ch1, probe A,B) λ_{em}= 650-700nm (ch2, probe A)	emission ratio I_{ch2} / I_{ch1}	1-4	15 min (5 µM)	not determined	A549 cells		[17]

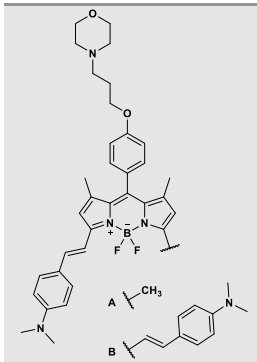	λ_{em}= 675-725nm (ch2, probe B)							
BODIPY- rhodamine-based probes 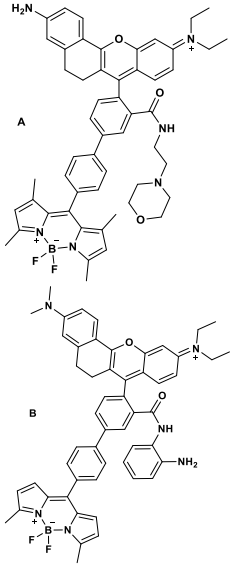	λ_{ex}=430-500 nm (donor) λ_{em}= 500-550nm (ch1, donor) λ_{em}= 625-675nm (ch2, acceptor)	emission ratio I_{ch2} / I_{ch1} (lower pH range) or I_{ch1} / I_{ch2} (higher pH range)	3-6.5 (probe A) 2.5-7 (probe B)	30 min (5-15 µM)	not determined	HeLa cells	FRET-based	[18]
hemicyanine-based probe	λ_{ex}=600-700 nm λ_{em}= 650-680nm (ch1) λ_{em}= 690-720nm (ch2)	emission ratio I_{ch1} / I_{ch2} (appr. 670 nm / 708 nm)	4-6	5 min (50 nM)	not determined	MCF-7 cells, HeLa cells		[19]

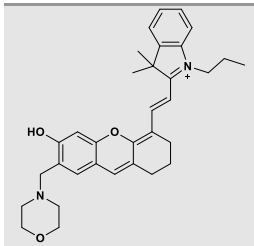								
lanthanide probes 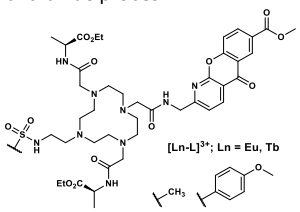	λ_{ex}=355 nm λ_{em}= 450-570nm (Tb) λ_{em}= 605-720nm (Eu)	emission ratio I_{Tb} / I_{Eur}	5-7	1-3 h (30-200 µM)	not determined	several cell lines (NIH-3T3,CHO,PC3, MCF7, HeLa)	ratiometric imaging performed with mixture of Tb and Eur complexes of L^2	20
spirocyclic rhodamine-lactam-based probes 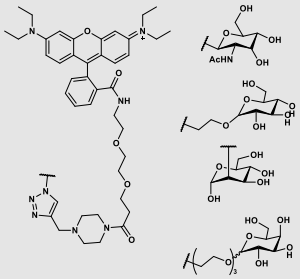	λ_{ex}= 480 nm λ_{em}= 550-650nm	emission intensity at appr. 580 nm increased in protonated form	4-7	45 min (1 µM)	after 2 h superior retention compared to LysoTracker™ Green, retention observed for 48 h	several cell lines		21
rhodamine-based probe 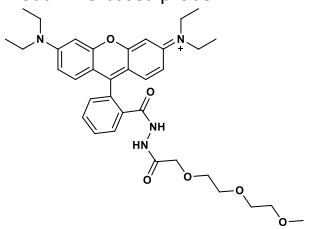	λ_{ex}=525-560 nm λ_{em}= 560-630nm	emission intensity at 578 nm increased in protonated form	4.5-7	30 min (10 µM)	not determined	several cell lines (MCF-7, HeLa, Raw 264.7)		22
rhodamine-based probe	λ_{ex}=563 nm λ_{em}= 570-650nm	emission intensity at 589 nm	4.5-7	3-12 h (1-5 µM)	not determined	HeLa cells		23

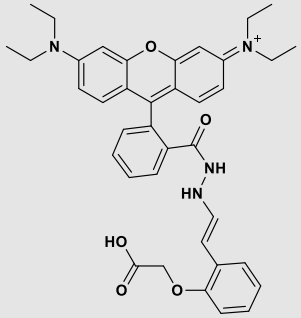		increased in protonated form						
rhodamine-based probes 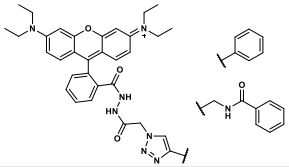	λ_{ex}=540-555 nm λ_{em}= 560-630nm	emission intensity at 583 nm increased in protonated form	4-6 (probe A) 4.4-6.5 (probe B)	30 min (5 µM)	not determined	HeLa cells		24
rhodamine-based probe 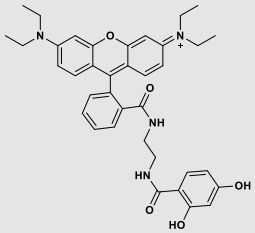	λ_{ex}=540 nm λ_{em}= 560-630nm	emission intensity at 586 nm increased in protonated form	3-6	30 min (5 µM)	not determined	several cell lines (MCF-7, HepG2)	additional live cell imaging in mice showing tissue with decreased pH	25
rhodamine-based probe 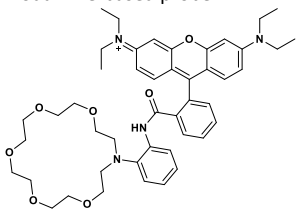	λ_{ex}=550 nm λ_{em}= 560-640nm	emission intensity at 588 nm increased in protonated form	3-6.5	30 min (3 µM)	not determined	HeLa cells		26
rhodamine-based probe	λ_{ex}=600 nm λ_{em}=620-730 nm	emission intensity at 650 nm increased in protonated form	4.5-6	20-30 min (1-4 µM)	not determined	HeLa cells		27

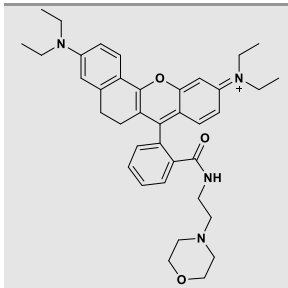							
spirocyclic probes 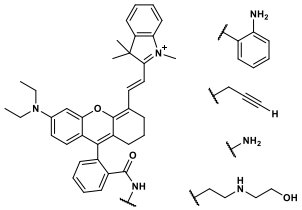	λ_{ex}=635 nm λ_{em}=700-800 nm	emission intensity at 743 nm increased in protonated form	4-7	2 h (5-20 μM)	not determined	several cell lines (MDA-MB-231, HUVEC)	[28]
Quinoline-benzothiazole probe 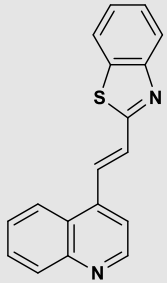	λ_{ex}=300-405 nm λ_{em}=410-480 nm	emission intensity at 428 nm decreased in protonated form	3-5	20 min (10 μM)	not determined	several cell lines (HeLa, HepG2)	[29]
galactosyl naphthalimide-piperazine probe	λ_{ex}=390-430 nm λ_{em}=500-600 nm	emission intensity at 530 nm increased in protonated form	5-8	40 min (20 μM)	not determined	HepG2 cells	[30]

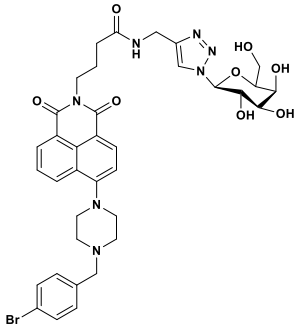								
NBD-based probe 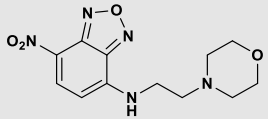	λ_{ex}=445 nm λ_{em}=500-600 nm	emission intensity at 530 nm increased in protonated form	3-6	30-120 min (1-10 µM)	not determined	HeLa cells		[31]
naphthalimide-based probe 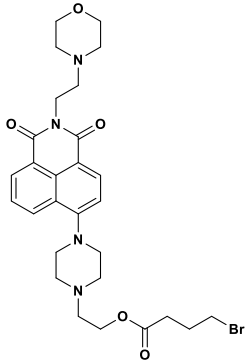	λ_{ex}=450-488 nm λ_{ex}=800 nm (two photon exc.) λ_{em}=500-600 nm	emission intensity at 531 nm increased in protonated form	4-8	30 min (2 µM)	not determined	HeLa cells	two-photon excitation possible	[32]
dicyanoisophorone-based probe 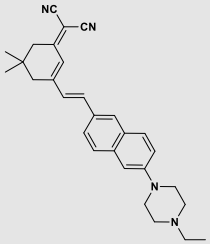	λ_{ex}=400-500 nm λ_{em}=600-800 nm	emission intensity at 730nm increased in protonated form	4-8	30 min (10 µM)	not determined	HeLa cells		[33]
Darrow Red-based probes	λ_{ex}=570 nm	emission intensity	2-4 (probe A)	10-15min (10 µM)	not determined	several cell lines		[34]

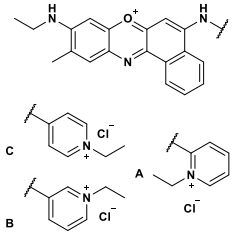	λ_{em}=580-850 nm	at appr. 660-670 nm increased in protonated form	5-7 (probe B) 6-9 (probe C)			(HeLa, KB, VL79)	
BODIPY-based probes 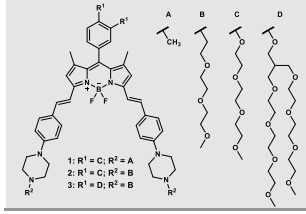	λ_{ex}=600-700 nm λ_{em}=650-850 nm	emission intensity at 715nm increased in protonated form	2.5-6	2 h (5 µM)	not determined	several cell lines (MDA-MB-231, HUVEC)	35

Table S2: TD-ωPBEhPBE/6-31G(d)/PCM(DMSO) calculated wavelengths (λ, nm) and oscillator strengths (f) of the LW-AT of the stable conformers of imino-NMI-LS(+) and imino-NMI-LS(2+)

	Imino-NMI-LS(+)				Imino-NMI-LS(2+)	
Conformer	**1**	**2**	**3**	**4**	**1**	**2**
λ	474	476	478	474	470	463
f	0.0018	0.0008	0.0021	0.0022	0.0002	0.0001

Table S3: Calculated extinction coefficients of different bands in the absorbance spectra of NMI-LS in buffers of different pH. Data are given as λ_{max} in nm (ε in $mol^{-1}dm^3cm^{-1}$)

pH	band 1	band 2	band 3
1.4	463.5 (8215)	431.5 (17649)	413.0 (17203)
2.4	463.5 (12657)	433.0 (17724)	413.0 (15652)
3.1	463.5 (16064)	436.5 (16465)	413.0 (13477)
3.7	463.5 (21232)	437.5 (18150)	
4.1	463.5 (21994)	437.5 (16743)	
4.4	463.5 (23510)	440.0 (16710)	
4.6	463.5 (27121)	440.0 (19351)	
4.9	463.5 (28117)		
5.4	463.5 (28115)		
6.5	463.5 (28108)		
7.5	463.5 (25574)		
8.3	465.0 (22892)		
10.7	463.5 (23577)		

Table S4: Fit results for the determination of pK_a' according to equation 3 (main document) and estimation of pK_a from intensity values of maximal protonation/ deprotonation determined for the excitation ratios 462 nm /413 nm, 458 nm /405 nm and the emission ratios 467 nm/449 nm according to equation 2 (main document).

	excitation ratio 462 nm/413 nm	excitation ratio 458 nm/405 nm	emission ratio 467 nm/449 nm
pK_a'	4.33	4.39	5.33
R_{min}	0.12	0.08	0.86
R_{max}	5.44	6.50	14.31
c	1.34	1.28	1.73
$\log(I_a/I_b)$	1.03	1.18	2.19
estimated pK_a	3.3	3.21	3.14

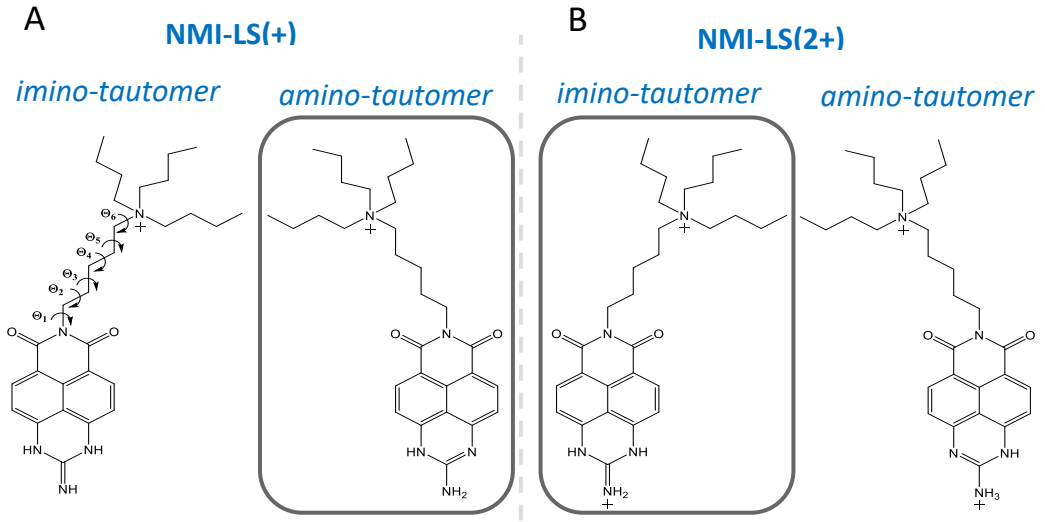

Figure S1: Chemical structures of the imino (left in each half) and of the amino (right in each half) tautomer of NMI-LS in its (**A**) deprotonated and (**B**) protonated form used for the DFT calculations; the more stable tautomer of each form is framed; the torsion angles rotated during the conformational search are denoted on imino-NMI-LS(+).

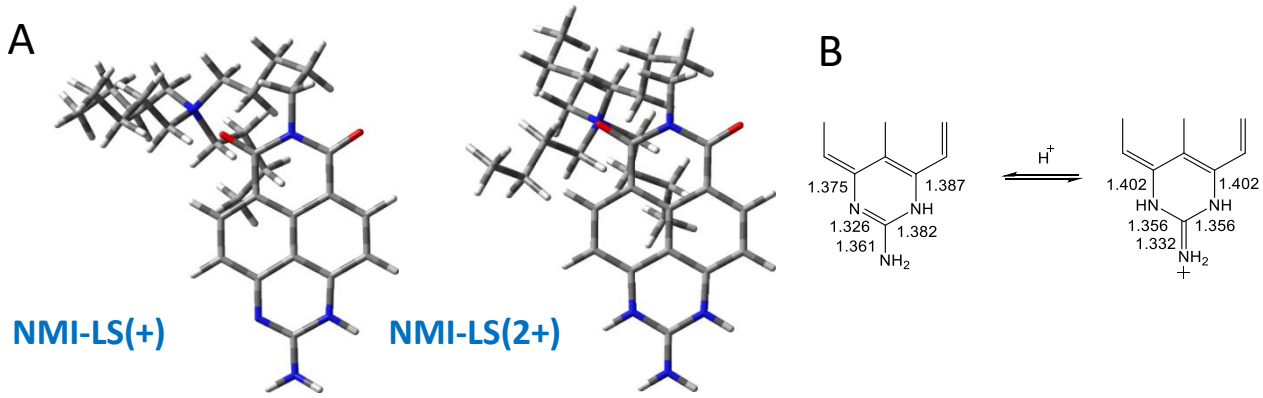

Figure S2: (A) Optimized geometries of the most stable tautomers of NMI-LS(+) (left) and NMI-LS(2+) (right), which were used for calculation of the absorption transitions and (**B**) electron density redistribution causing the hypsochromic shift of the longest-wavelength electronic transition upon protonation

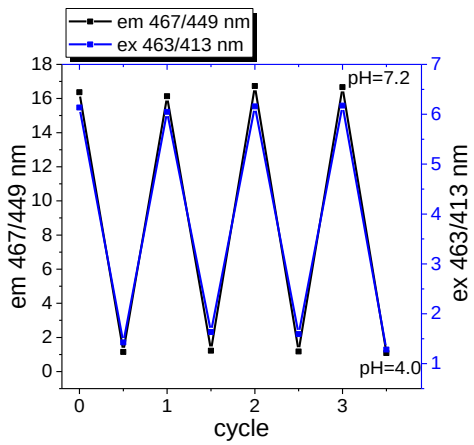

Figure S3: Reversibility of spectral changes at different pH values. Ratios of fluorescence intensity of emission peaks 467/449 nm (black squares) and excitation peaks 463/413 nm (blue diamonds) remain constant after several cycles of pH shifts.

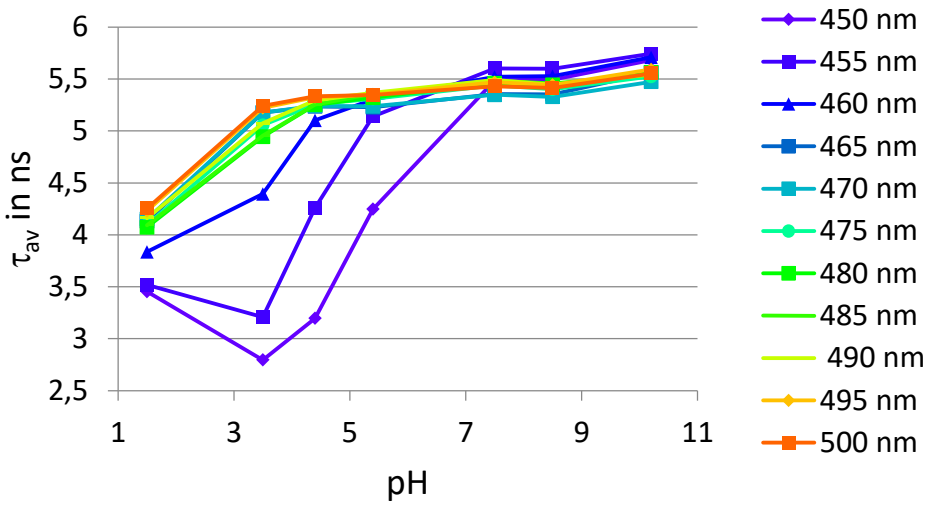

Figure S4. Time-resolved emission of NMI-LS (3 µM) in buffers of different pH values. Fluorescence lifetimes of NMI-LS at different pH values and emission wavelengths (λ_{ex}=440 nm), biexponential fit; $\tau_{av}=a_1\tau_1+a_2\tau_2$.

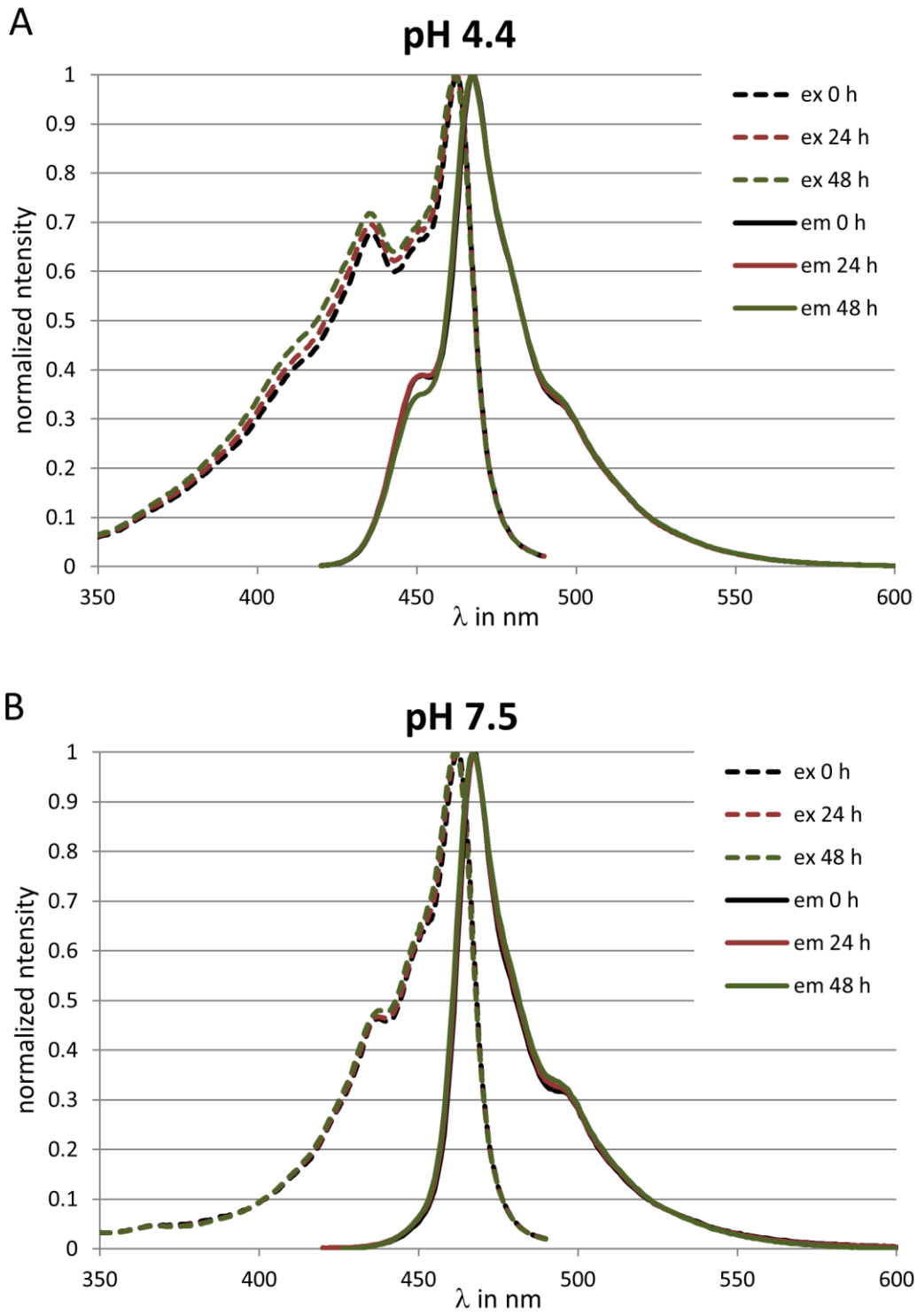

Figure S5 Fluorescence excitation (dashed lines) and emission (solid lines) spectra of NMI-LS in aqueous buffer after incubation for a time period of 48 h at 37°C. A) pH 4.4 or B) pH 7.5.

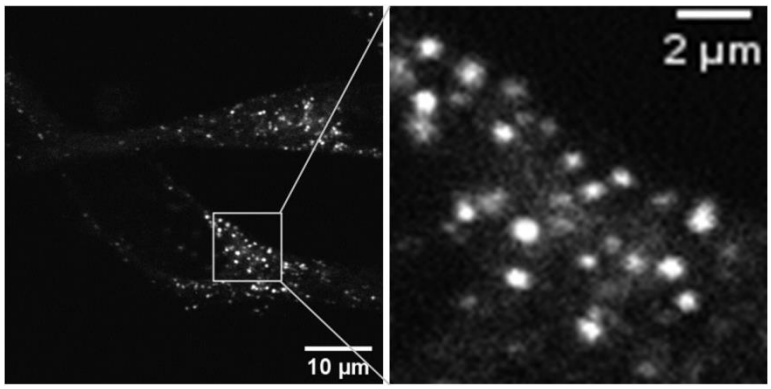

Figure S6. NMI-LS-labeled HeLa cells imaged using two-photon excitation at 900 nm. The right panel shows a magnified view of the area indicated by a square in the left panel.

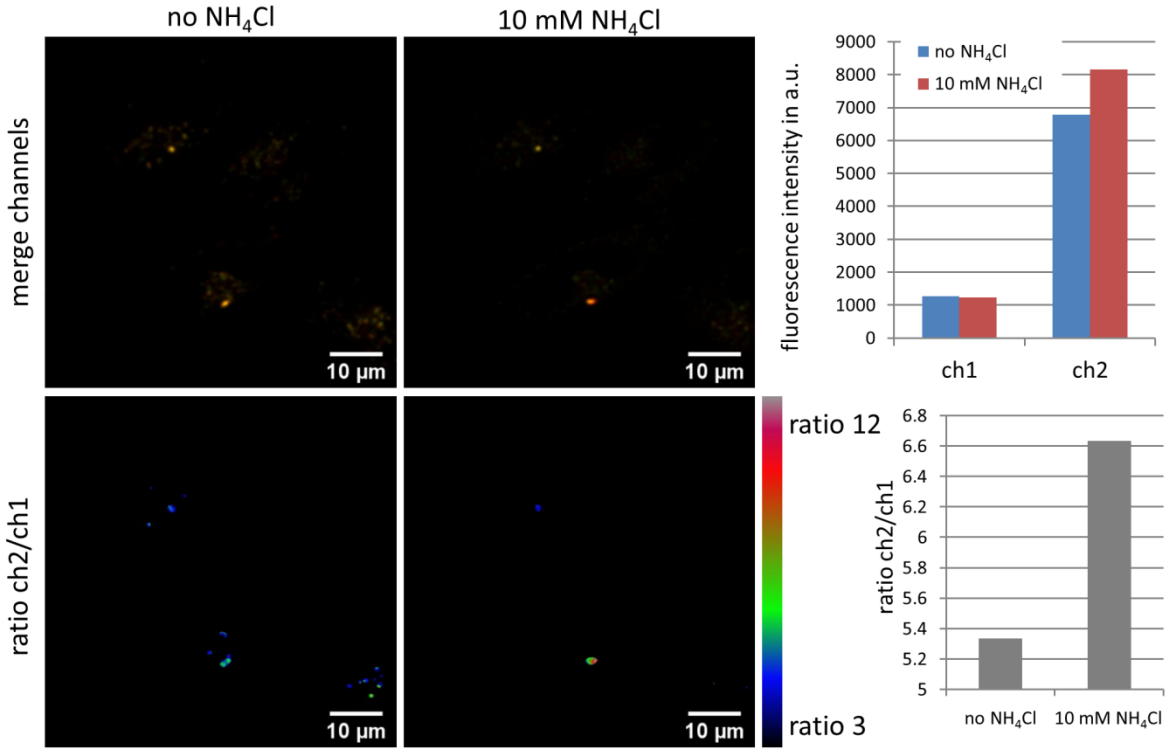

Figure S7. Ratiometric emission before and 2.5 min after the addition of 10 mM ammonium chloride. The sample was imaged using two-photon excitation at 880 nm. Emission was monitored from 410-455 nm (ch1, green) and 466-518 nm (ch2, red). The lower panels show the ratio between emission of ch2/ch1. An increase in the pH is visualized by an increase in this ratio.

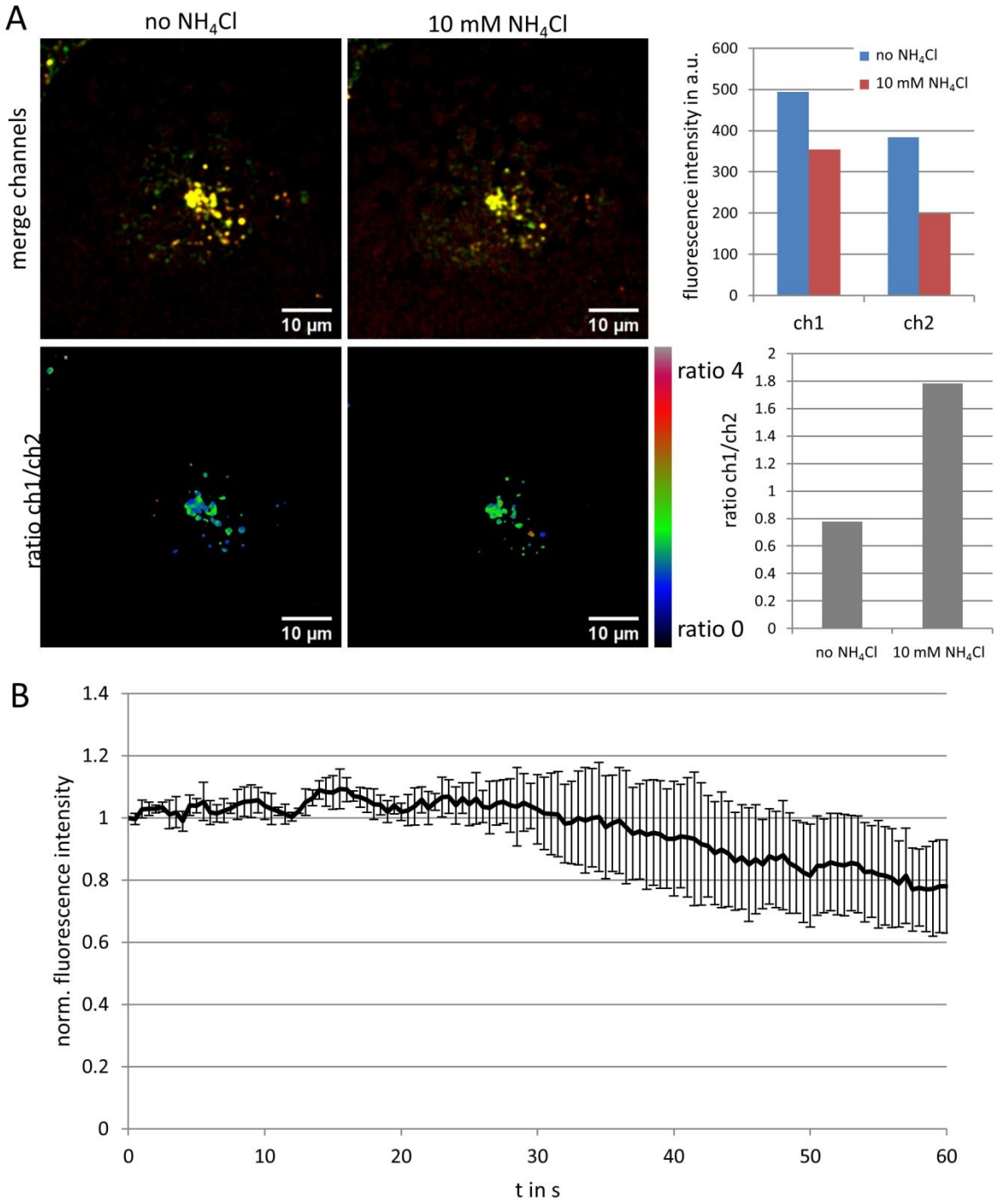

Figure S8. A) Ratiometric emission scan of the commercial LSYB dextran before and 2 min after the addition of 10 mM ammonium chloride. The sample was imaged using two-photon excitation at 730 nm. Emission was monitored from 419-499 nm (ch1, green) and 517-624 nm (ch2, red). The lower panels show the ratio between emission of ch1/ch2. An increase in the pH is visualized by an increase in this ratio. B) Photostability of LSYB upon excitation at 720 nm, 14.4 mW. Time lapse images (1024 x 1024 pixels) were acquired in 3 FOV for 60 min every 30 s with a pixel dwell time of 1.58 µs Data represent mean ± standard deviation of background-corrected intensity of 3 FOV normalized to the first acquired image.

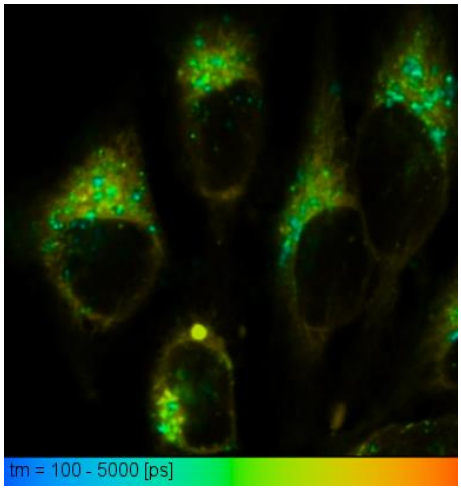

Figure S9 Average fluorescence lifetimes of NMI-LS in HeLa cells (two-photon excitation λ_{ex}=900 nm , 80 MHz, λ_{em}=430-490 nm), biexponential fit; $\tau_{Av}=a_1\tau_1+a_2\tau_2$.

References

1. D. Uersfeld, S. Stappert, C. Li and K. Mullen, *Adv Synth Catal*, 2017, **359**, 4184-4189.
2. S. Kaloyanova, Y. Zagranyarski, S. Ritz, M. Hanulova, K. Koynov, A. Vonderheit, K. Mullen and K. Peneva, *J Am Chem Soc*, 2016, **138**, 2881-2884.
3. S. Ohkuma and B. Poole, *Proc Natl Acad Sci U S A*, 1978, **75**, 3327-3331.
4. M. J. Geisow, *Exp Cell Res*, 1984, **150**, 29-35.
5. I. Eriksson, K. Öllinger and H. Appelqvist, in *Lysosomes: Methods and Protocols*, eds. K. Öllinger and H. Appelqvist, Springer New York, New York, NY, 2017, DOI: 10.1007/978-1-4939-6934-0_11, pp. 179-189.
6. E. Zhang, S. Wang, X. Su and S. Han, *Analyst*, 2020, DOI: 10.1039/c9an02441g.
7. H. J. Kim, C. H. Heo and H. M. Kim, *J Am Chem Soc*, 2013, **135**, 17969-17977.
8. T. Zhang, D. Xu, C. Y. Poon, X. Wang, F. Bolze, H. W. Li and M. S. Wong, *Talanta*, 2019, **202**, 34-41.
9. X. J. Zhao, C. Wang, G. Q. Yuan, H. Y. Ding, L. Y. Zhou, X. G. Liu and Q. L. Lin, *Sensor Actuat B-Chem*, 2019, **290**, 79-86.
10. G. Q. Yuan, H. Y. Ding and L. Y. Zhou, *Spectrochim Acta A*, 2020, **224**.
11. X. F. Zhang, T. Zhang, S. L. Shen, J. Y. Miao and B. X. Zhao, *J Mater Chem B*, 2015, **3**, 3260-3266.
12. G. Li, D. Zhu, L. Xue and H. Jiang, *Org Lett*, 2013, **15**, 5020-5023.
13. B. L. Dong, X. Z. Song, C. Wang, X. Q. Kong, Y. H. Tang and W. Y. Lin, *Analytical Chemistry*, 2016, **88**, 4085-4091.
14. X. J. Liu, Y. A. Su, H. H. Tian, L. Yang, H. Y. Zhang, X. Z. Song and J. W. Foley, *Analytical Chemistry*, 2017, **89**, 7038-7045.
15. J. H. Zhang, M. L. Zhu, J. W. Cui, C. M. Wang, Z. W. Zhou, T. H. Wang, L. Gong, C. R. Su, D. D. Qi, Y. Z. Bian, H. W. Du and J. Z. Jiang, *J Photoch Photobio A*, 2020, **396**.
16. Z. W. Xue, H. Zhao, J. Liu, J. H. Han and S. F. Han, *Acs Sensors*, 2017, **2**, 436-442.
17. M. L. Zhu, P. P. Xing, Y. B. Zhou, L. Gong, J. H. Zhang, D. D. Qi, Y. Z. Bian, H. W. Du and J. Z. Jiang, *J Mater Chem B*, 2018, **6**, 4422-4426.
18. S. Xia, M. X. Fang, J. B. Wang, J. H. Bi, W. Mazi, Y. B. Zhang, R. L. Luck and H. Y. Liu, *Sensor Actuat B-Chem*, 2019, **294**, 1-13.
19. Q. Q. Wan, S. M. Chen, W. Shi, L. H. Li and H. M. Ma, *Angew Chem Int Edit*, 2014, **53**, 10916-10920.
20. D. G. Smith, B. K. McMahon, R. Pal and D. Parker, *Chem Commun (Camb)*, 2012, **48**, 8520-8522.
21. X. Chen, Y. Bi, T. Wang, P. Li, X. Yan, S. Hou, C. E. Bammert, J. Ju, K. M. Gibson, W. J. Pavan and L. Bi, *Sci Rep*, 2015, **5**, 9004.
22. H. Zhu, J. L. Fan, Q. L. Xu, H. L. Li, J. Y. Wang, P. Gao and X. J. Peng, *Chem Commun*, 2012, **48**, 11766-11768.
23. H. S. Lv, S. Y. Huang, Y. Xu, X. Dai, J. Y. Miao and B. X. Zhao, *Bioorg Med Chem Lett*, 2014, **24**, 535-538.
24. K. K. Yu, K. Li, J. T. Hou, H. H. Qin, Y. M. Xie, C. H. Qian and X. Q. Yu, *Rsc Adv*, 2014, **4**, 33975-33980.
25. B. Li, G. B. Ge, L. L. Wen, Y. Yuan, R. Zhang, X. J. Peng, F. Y. Liu and S. G. Sun, *Dyes Pigments*, 2017, **139**, 318-325.
26. D. Lee, K. M. K. Swamy, J. Hong, S. Lee and J. Yoon, *Sensor Actuat B-Chem*, 2018, **266**, 416-421.
27. G. L. Niu, P. P. Zhang, W. M. Liu, M. Q. Wang, H. Y. Zhang, J. S. Wu, L. P. Zhang and P. F. Wang, *Analytical Chemistry*, 2017, **89**, 1922-1929.
28. G. K. Vegesna, J. Janjanam, J. H. Bi, F. T. Luo, J. T. Zhang, C. Olds, A. Tiwari and H. Y. Liu, *J Mater Chem B*, 2014, **2**, 4500-4508.
29. L. Fan, M. Nan, J. Y. Ge, X. D. Wang, B. Lin, W. J. Zhang, S. M. Shuang and C. Dong, *New J Chem*, 2018, **42**, 13479-13485.
30. Y. X. Fu, J. J. Zhang, H. Wang, J. L. Chen, P. Zhao, G. R. Chen and X. P. He, *Dyes Pigments*, 2016, **133**, 372-379.
31. X. J. Cao, L. N. Chen, X. Zhang, J. T. Liu, M. Y. Chen, Q. R. Wu, J. Y. Miao and B. X. Zhao, *Anal Chim Acta*, 2016, **920**, 86-93.
32. C. Wang, B. L. Dong, X. Q. Kong, N. Zhang, W. H. Song and W. Y. Lin, *Luminescence*, 2018, **33**, 1275-1280.
33. W. Shen, L. Wang, S. Zhu, S. Yu, C. Cai, W. Yi and Q. Zhu, *Anal Biochem*, 2020, **596**, 113609.
34. D. D. He, W. Liu, R. Sun, C. Fan, Y. J. Xu and J. F. Ge, *Analytical Chemistry*, 2015, **87**, 1499-1502.
35. J. T. Zhang, M. Yang, C. Li, N. Dorh, F. Xie, F. T. Luo, A. Tiwari and H. Y. Liu, *J Mater Chem B*, 2015, **3**, 2173-2184.